Carbohydrate Polymers 80 (2010) 291–295

Contents lists available at ScienceDirect

Carbohydrate Polymers

journal homepage: www.elsevier.com/locate/carbpol

Effect of the degree of deacetylation on the thermal decomposition of chitin and chitosan nanofibers

Young Sik Nam [a], Won Ho Park [a,*], Daewoo Ihm [b], Samuel M. Hudson [c]

[a] Department of Advanced Organic Materials and Textile System Engineering and BK21 FTIT, Chungnam National University, Daejeon 305-764, South Korea
[b] Department of Chemical Engineering, Hoseo University, Asan City, Chungnam 336-795, South Korea
[c] Department of Fiber and Polymer Science, College of Textiles, North Carolina State University, Raleigh, NC 27695-8301, USA

ARTICLE INFO

Article history:
Received 25 September 2009
Received in revised form 14 November 2009
Accepted 18 November 2009
Available online 22 November 2009

Keywords:
Chitosan
Chitin
Nanofibers
Degree of deacetylation
Thermal decomposition

ABSTRACT

Chitin and chitosan nanofibers with different degrees of deacetylation (DD) were fabricated by electrospinning using 1,1,1,3,3,3-hexafluoro-2-propanol (HFIP) as the spinning solvent and by subsequent deacetylation using a 40% aqueous NaOH solution at 100 °C for 0–150 min. The thermal decomposition behavior of the chitin and chitosan nanofibers was examined by thermogravimetric analysis (TGA) and differential scanning calorimetry (DSC). The thermal stability of the chitin/chitosan nanofibers was decreased with increasing the DD and the peak temperature for thermal decomposition on the TGA curves was shifted to a lower temperature. The activation energies for the thermal degradation of the chitin/chitosan nanofibers were calculated from the TGA curves. The two exotherms corresponding to the decomposition of *N*-acetyl-D-glucosamime and D-glucosamine units in the chitin/chitosan molecular chains were observed on the DSC thermograms. This suggests that the residual *N*-acetyl groups had a blocky distribution in the molecular chain, possibly due to heterogeneous deacetylation.

1. Introduction

Chitin is a polysaccharide composed of (1,4)-linked *N*-acetyl-β-D-glucosamine that is obtained primarily from shrimp and crab shells. It is the second most abundant natural polymer in the world next to cellulose. It has been estimated that 10^{10}–10^{12} tons of chitin are biosynthesized each year (Percot, Viton, & Domard, 2003). Chitin can be converted to its *N*-deacetylated product, i.e., chitosan, which has a repeated structure of (1,4)-linked β-D-glucosamine, by homogeneous or heterogeneous alkaline *N*-deacetylation. The degree of deacetylation (DD, %) is defined as the ratio of *N*-deacetylated (amino) groups to *N*-acetyl groups at the C2 position in the backbone. The physical, chemical and biological properties of chitin or chitosan are strongly dependent on its DD value. Chitin and/or chitosan has several distinctive biological properties, including biocompatibility and biodegradability, cellular binding capability, acceleration of wound healing, hemostatic properties, and anti-bacterial properties (Cho, Cho, Chung, Yoo, & Ko, 1999; Muzzarelli, 1993; Tomihata & Ikada, 1997). Therefore, they have been used extensively in many biomedical applications, such as cosmetics, medical materials for human health and food additives. In particular, chitosan can be used in a large variety of physical forms, including beads, films, sponges, tubes, powders and fibers because it is quite soluble under acidic aqueous conditions (Rinaudo, 2006).

Electrospinning is a unique technique to produce polymer nanofibers using a high electric potential and is applicable to most polymers. Polymer nanofibrous structures, with several useful properties, such as a high specific surface area and high porosity, are of considerable interest for various applications, including fiber membranes for filter applications (Gibson, Schreuder-Gibson, & Rivin, 2001), biomedical applications, such as wound dressings and scaffolds for tissue engineering (Kenawy et al., 2003; Li, Laurencin, Caterson, Tuan, & Ko, 2002; Min et al., 2004a, 2004b; Yoshimoto, Shin, Terai, & Vacanti, 2003), and sensing applications (Athreya & Martin, 1999; Wang et al., 2002). Unfortunately, chitosan is difficult to electrospin into a nanofibrous structure owing to its polycationic character in an acidic aqueous solution as a result of the many amino groups in its backbone. Until now, nanofibrous structures were generated successfully by electrospinning chitosan solutions in 90 wt.% aqueous acetic acid (Geng, Kwon, & Jang, 2005) or by using a solvent like trifluoroacetic acid (TFA) or TFA/dichloromethane (DCM) (Ohkawa, Cha, Kim, Nishida, & Yamamoto, 2004). However, electrospinning conditions are relatively limited in terms of concentration, molecular weight, and DD (Vrieze, Westbroek, Camp, & Langenhove, 2007).

On the other hand, chitin or chitosan can be depolymerized by a variety of degradation processes, including acid-catalyzed, alkaline-catalyzed and enzymatic hydrolysis. In general, the degradation of

* Corresponding author. Tel.: +82 42 821 6613; fax: +82 42 823 3736.
E-mail address: parkwh@cnu.ac.kr (W.H. Park).

0144-8617/$ - see front matter © 2009 Elsevier Ltd. All rights reserved.
doi:10.1016/j.carbpol.2009.11.030

chitin or chitosan occurs via the cleavage of glycosidic linkages. However, there a fewer reports on the thermal degradation process of chitin/chitosan and its derivatives than on chemical and enzymatic degradation (De Britto & Campana-Filho, 2004; Holme, Foros, Pettersen, Dornish, & Smidsrod, 2001; Hong et al., 2007; Neto et al., 2005; Qu, Wirsen, & Albertsson, 2000; Wanjin, Cunxin, & Donghua, 2005). Furthermore, the thermal degradation of chitin or chitosan with a broad range of DD has received little attention (Guinesi & Cavalheiro, 2006; Kittur, Prashanth, Sankar, & Tharanathan, 2002). Kittur et al. (2002) examined the thermal transitions of chitin, chitosan and their carboxymethyl derivatives using differential scanning calorimetry (DSC). There is a good correlation between the area/height of the decomposition peaks on DSC thermograms and the DD/degree of substitution (DS). Guinesi and Cavalheiro (2006) also proposed that the area and height of the decomposition peaks on the DSC curves can be used as an analytical method to determine the DD of chitin/chitosan. These studies focused mainly on correlating the change in the DSC thermograms due to the thermal decomposition of chitin/chitosan with different DD, without examining the kinetics on the thermal decomposition process.

In a previous study, chitin and chitosan nanofibers with various degrees of DD could be fabricated from the deacetylation of electrospun chitin fibers using 1,1,1,3,3,3-hexafluoro-2-propanol (HFIP) as a solvent (Min et al., 2004a, 2004b). This study examined the thermal degradation of the nanofibrous chitin and chitosan with a broad range of DD using thermogravimetric analysis (TGA) and differential scanning calorimetry (DSC).

2. Experimental

2.1. Materials

Chitin powder (M_w = 920,000, DD = 8%) was supplied by Kumho Chemical Products Co. (Korea). To enhance the solubility, the chitin powder was packed into polyethylene bags and irradiated with Co^{60} γ rays (Korea Atomic Energy Research Institute, Daejeon, Korea) with an energy of 200 kGy. The MW of the irradiated chitin powder determined by dilute solution viscometry was 91,000 (Min et al., 2004a, 2004b). 1,1,1,3,3,3-hexafluoro-2-propanol (HFIP) was purchased from Sigma–Aldrich (USA). All reagents were of analytical grade and used as received.

2.2. Electrospinning of chitin

Chitin solutions were prepared by dissolving the irradiated chitin powders (M_w = 91,000) in HFIP for 3 days. The concentration of the chitin solutions used for electrospinning ranged from 5% by weight. In the electrospinning process, a high electric potential was applied to a droplet of a chitin solution at the tip (0.495 mm in internal diameter) of a syringe needle. The electrospun chitin nanofibers were collected on a target drum placed 7 cm from the syringe tip. A voltage of 17 kV was applied to the collecting target using a high voltage power supply (Chungpa EMT Co., Korea).

2.3. Deacetylation of electrospun chitin fibers

The as-spun chitin nanofibers (1.0 g) were refluxed in a 40% NaOH aqueous solution (50 mL) for 30–150 min at 100 °C under a nitrogen atmosphere, washed with distilled water, and dried under vacuum for 24 h. The DD of the *N*-deacetylated products was calculated using the integrals of the peak due to three protons of a *N*-acetyl group at 2.0 ppm and a peak due to the proton at C2 at 3.5 ppm on the ^{1}H NMR spectrum (Lavertu et al., 2003). The DD of the initial chitin nanofibers was calculated using the peak areas at 22 ppm (methyl carbon) and 50–105 ppm (C2–C6 carbons) of the solid state ^{13}C CP/MAS NMR spectrum (Tolaimate et al., 2000).

2.4. Measurement and characterizations

The thermal properties were measured by differential scanning calorimetry (DSC, PerkinElmer DSC-7) and thermogravimetric analysis (TGA, PerkinElmer TGA-7). For the DSC and TGA analyses, the samples were heated to 300 and 500 °C, respectively, at a heating rate of 10 °C/min under a nitrogen flow. The morphology of the electrospun and deacetylated chitin fibers was observed by scanning electron microscopy (SEM) (Hitachi S-2350, Japan) after coating the sample with gold. The average fiber diameter was determined by analyzing the SEM images using a custom code image-analysis program (Scope Eye II).

3. Results and discussion

3.1. Electrospinning and deacetylation of chitin nanofibers

The DD of chitin and chitosan has a significant effect on the physicochemical properties of their fibers. For example, the solubility and structural change in chitin have a close relationship with the DD value and the means of deacetylation, i.e., heterogeneous or homogeneous alkaline hydrolysis. In this study, the heterogeneous deacetylation reaction of chitin nanofibers was carried out in a concentrated NaOH aqueous solution (40%) at 100 °C. The chitosan nanofibers with different DDs were generated from the chitin nanofibers by a heterogeneous alkaline treatment. Fig. 1 shows the change in DD as a function of the deacetylation time. The DD increased rapidly to 60% within 30 min, and increased slowly to 85%. The rate of the deacetylation reaction using chitin nanofibers was very fast, particularly in the early stages, possibly because they have a high surface area and less compact structure with low crystallinity. Fig. 2 shows SEM images and the diameters of chitin (DD = 8%) and deacetylated chitin (chitosan, DD = 85%) nanofibers before and after the NaOH treatment for 150 min at 100 °C. The chitin nanofibers were slightly swollen during deacetylation reaction under aqueous NaOH solution. However, there were no significant morphological changes in the chitin nanofibers observed after the NaOH treatment, even though a slight increase in fiber diameter occurred from 163 nm (chitin, DD = 8%) to 180 nm (chitosan, DD = 85%).

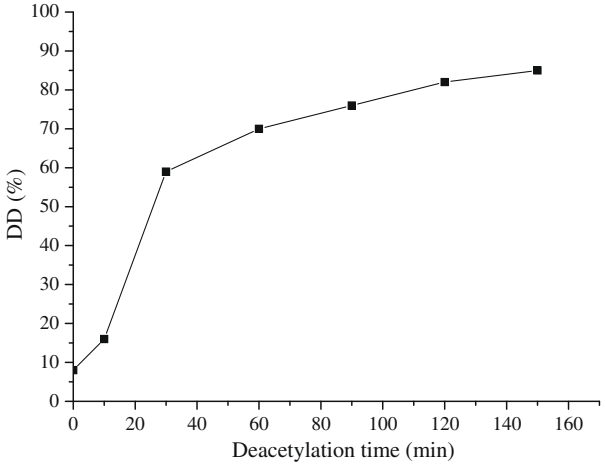

Fig. 1. Changes in the degree of deacetylation (DD) as a function of the reaction time.

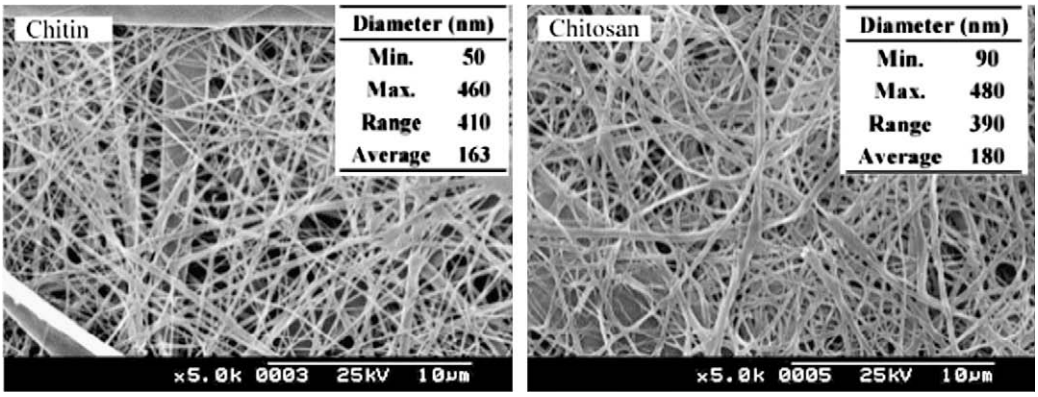

Fig. 2. SEM images of the chitin (DD = 8%) and deacetylated chitin (chitosan, DD = 85%) nanofibrous matrix, before and after the deacetylation reaction.

3.2. Thermal degradation behavior of chitin and chitosan nanofibers

Fig. 3 shows the TGA and corresponding DTG thermograms of the chitin and chitosan nanofibers with different DD. Overall, the maximum degradation temperatures decreased from ~330 to ~270 °C with increasing the DD of chitin. This result suggests that the chitin nanofibers had been converted completely to chitosan nanofibers. The thermal decomposition of electrospun chitin or chitosan nanofibers occurred at lower temperature range (20–30 °C) than bulk chitosan or chitin with the corresponding DDs (Guinesi & Cavalheiro, 2006; Wanjin et al., 2005). This difference might be mainly attributed to a higher surface area of chitin (chitosan) nanofibers. The lower maximum degradation temperature of the chitosan nanofibers might be the result of a decrease in thermal stability due to the decreased *N*-acetyl content and crystallinity (Wanjin et al., 2005). The thermal degradation pattern of the chitosan (DD > 50%) nanofibers occurred in two stages with two maximum rate peaks in the differential thermogravimetric (DTG) curves, whereas the thermal decomposition of chitin nanofibers followed a single-step degradation reaction, as shown in Fig. 3b. Table 1 lists the initial (T_i) and maximum (T_{max}) decomposition temperatures of the chitin and chitosan nanofibers with different DD. The first maximum decomposition temperature of chitosan nanofibers, which is associated with the degradation reaction of 2-amino-2-deoxy-D-glucopyranose (GlcN) units, increased gradually from ~235 to ~244 °C with increasing DD. The second maximum decomposition temperature of chitosan nanofibers corresponding to the degradation of 2-acetamido-2-deoxy-D-glucopyranose (GlcNAc) units decreased from 341 to 273 °C with increasing DD.

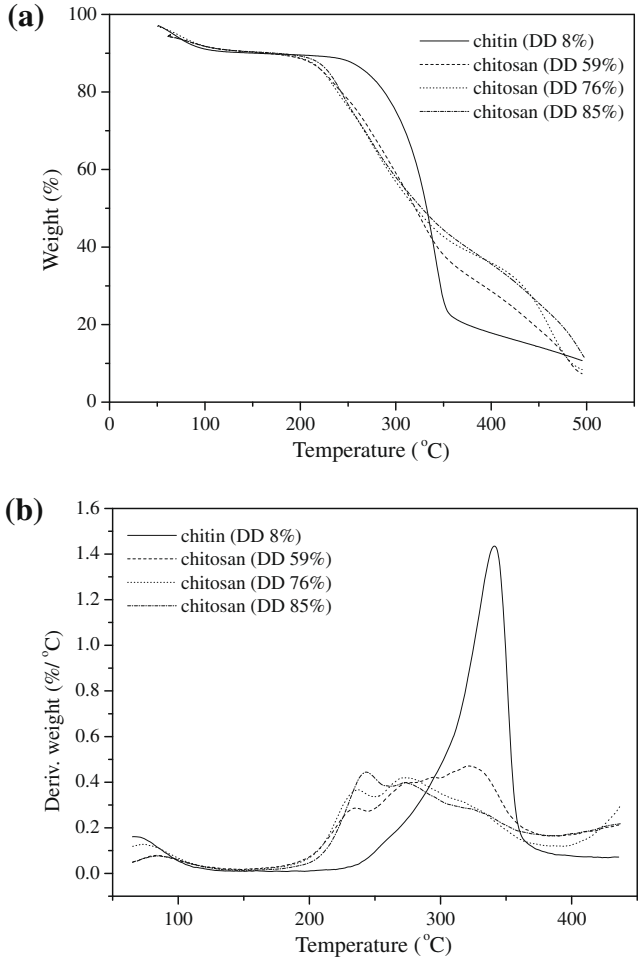

Fig. 3. TGA (a) and DTG (b) thermograms of the chitin nanofibers and its deacetylated chitin (chitosan) nanofibers.

The activation energy (E_a) for the thermal degradation of chitin and chitosan nanofibers was calculated from the TGA curves, using the Horowitz and Metzger method (Horowitz & Metzger, 1963) according to Eq. (1):

$$\mathrm{Ln}[\mathrm{Ln}(W_o/W_T)] = E_a\theta/RT^2_{max} \quad (1)$$

where W_o is the initial weight of the polymer, W_T is the residual weight of the polymer at temperature T, and θ is $T - T_{max}$. The activation energies were obtained from the slope (E_a/RT^2_{max}) of Ln[Ln(W_o/W_T)] vs. θ for the first and second stages of thermal decomposition, as shown in Fig. 4. The activation energies for the thermal degradation of all chitosan nanofibers (DD = 59–85%) were similar (~35 kJ/mol). The activation energy (~87 kJ/mol) of the chitin nanofibers was much higher than those (~35 kJ/mol) of the chitosan nanofibers because the *N*-acetylated units increased the thermal stability of the chitin molecular chains (Guinesi & Cavalheiro, 2006; Kittur et al., 2002).

Table 1
Parameters evaluated from the TGA and DTG thermograms of chitin and chitosan nanofibers.

Polymers	T_i[a] (°C)	T_{max1} (°C)	E_{a1} (kJ/mol)	T_{max2} (°C)	E_{a2} (kJ/mol)
Chitin (DD 8%)	152.2	–	–	341.2	87.0
Chitosan (DD 59%)	164.1	234.9	31.4	321.9	37.0
Chitosan (DD 76%)	165.4	237.2	37.9	271.9	36.9
Chitosan (DD 85%)	174.3	243.5	36.6	272.8	35.8

[a] Determined at 10% weight loss.

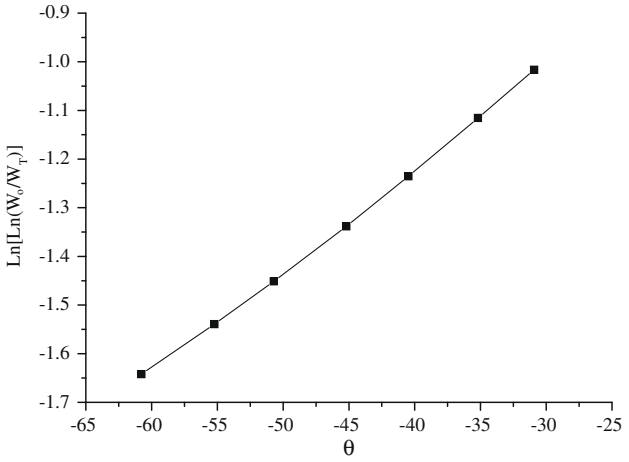

Fig. 4. Determination of the activation energy (E_a) for the thermal degradation of chitin nanofibers.

Fig. 5 shows the DSC thermograms of chitin/chitosan nanofibers with different DD. A broad endothermic peak in the range of 100–150 °C was observed in all chitin/chitosan nanofibers. This is related to the evaporation of water molecules in the nanofibers. With increasing DD, the area and position of the endothermic peaks was increased and shifted to a higher temperature, respectively. This suggests that chitosan nanofibers with a higher DD have higher water holding capacity and stronger interactions with water molecules. The chitin nanofibers showed the exothermic peak at ~363 °C due to the decomposition of *N*-acetyl (GlcNAc) units which is the main group in the backbone. For chitosan nanofibers with a 59% DD, two exothermic peaks were observed clearly at ~274 °C and ~362 °C due to the thermal decomposition of amino (GlcN) and *N*-acetyl (GlcNAc) residues, respectively. This indicates that the amino residues are less thermally stable than the *N*-acetyl ones. A similar thermal transition behavior was observed in the chitosan nanofibers with a DD of 76%. The chitosan nanofibers with a DD of 85% showed an exothermic peak at ~276 °C. The exothermic peak at higher temperature above 350 °C was not observed due to the low *N*-acetyl content. It should be noted that the peak area at approximately 275 °C increased with increasing DD and the peak area at approximately 360 °C decreased (Table 2). Heterogeneous deactylation occurred preferentially in the amorphous regions and continued more slowly from the surface to the center of the crystalline region, giving rise to a block structure in the backbone. This separated transition phenomenon was observed only in the products obtained from the heterogeneous deacetylation of chitin, which occurs in a block-like manner at the backbone. On the other hand, deacetylation occurs randomly at the backbone in the homogenous deactylation, and the two separate exothermic peaks due to the decomposition of amino (GlcN) and *N*-acetyl (GlcNAc) residues, respectively, were not observed.

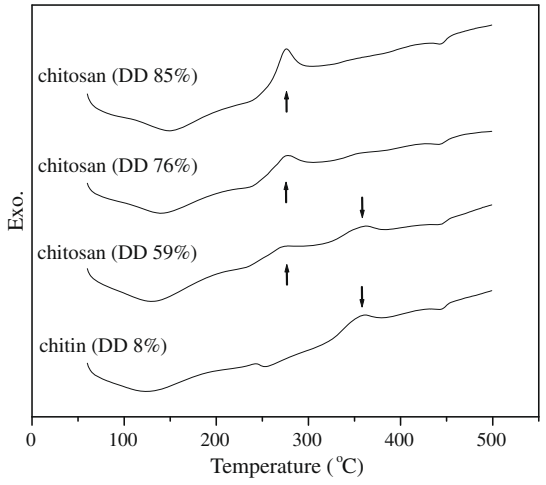

Fig. 5. DSC thermograms for the chitin and chitosan nanofibers with different DD.

Table 2
Thermal transitions of the chitin and chitosan nanofibers derived from the DSC thermograms.

Polymer	Exthotherm 1		Exthotherm 2	
	T_p (°C)	ΔH (J/g)	T_p (°C)	ΔH (J/g)
Chitin (DD 8%)	–	–	362.8	73.9
Chitosan (DD 59%)	273.7	51.5	362.4	60.8
Chitosan (DD 76%)	277.4	114.0	355.1	5.64
Chitosan (DD 85%)	276.3	160.1	–	–

4. Conclusion

Chitin and chitosan nanofibers with different DD were prepared by electrospinning and subsequent heterogeneous deacetylation using a concentrated alkaline solution. The thermal decomposition of chitin and chitosan nanofibers was examined by TGA and DSC. The thermal decomposition of the chitin nanofibers occurred in a single step, whereas the chitosan nanofibers with a DD > 50% showed a two-step degradation mechanism. The apparent activation energy and maximum decomposition temperature of the chitin nanofibers was higher than that of the chitosan nanofibers, possibly due to the higher thermal stability of the *N*-acetyl (GlcNAc) units. The separate decomposition of amino (GlcN) and *N*-acetyl (GlcNAc) units was observed clearly in the DSC thermograms. The two separate exothermic peaks in the DSC thermograms show that a block structure was obtained in the chitosan backbone by heterogeneous deacetylation.

Acknowledgment

This study was supported financially by the Biotechnology Development Program (Grant No. 850-20080090) funded by the Ministry of Education, Science, and Technology (MEST) of Korea.

References

Athreya, S. A., & Martin, D. C. (1999). Impedance spectroscopy of protein polymer modified silicon micromachined probes. *Sensors and Actuators, 72*, 203–216.
Cho, Y. W., Cho, Y. N., Chung, S. H., Yoo, G., & Ko, S. W. (1999). Water-soluble chitin as a wound healing accelerator. *Biomaterials, 20*, 2139–2145.
De Britto, D., & Campana-Filho, S. P. (2004). A kinetic study on the thermal degradation of *N*,*N*,*N*-trimethylchitosan. *Polymer Degradation and Stability, 84*, 353–361.
Geng, X., Kwon, O., & Jang, J. (2005). Electrospinning of chitosan dissolved in concentrated acetic acid solution. *Biomaterials, 26*, 5427–5432.
Gibson, P., Schreuder-Gibson, H., & Rivin, D. (2001). Transport properties of porous membranes based on electrospun nanofibers. *Colloids and Surfaces A, 187–188*, 469–481.
Guinesi, L. S., & Cavalheiro, E. T. G. (2006). The use of DSC curves to determine the acetylation degree of chitin/chitosan samples. *Thermochimica Acta, 444*, 128–133.
Holme, H. K., Foros, H., Pettersen, H., Dornish, M., & Smidsrod, O. (2001). Thermal depolymerization of chitosan chloride. *Carbohydrate Polymers, 46*, 287–294.
Hong, P. Z., Li, S. D., Ou, C. Y., Li, C. P., Yang, L., & Zhang, C. H. (2007). Thermogravimetric analysis of chitosan. *Journal of Applied Polymer Science, 105*, 547–551.
Horowitz, H. H., & Metzger, G. (1963). A new analysis of thermogravimetric traces. *Analytical Chemistry, 35*, 1464–1471.

Kenawy, E., Layman, J. M., Watkins, J. R., Bowlin, G. L., Matthews, J. A., Simpson, D. G., et al. (2003). Electrospining of poly(ethylene-co-vinyl alcohol) fibers. *Biomaterials, 24*, 907–913.

Kittur, F. S., Prashanth, K. V. H., Sankar, K. U., & Tharanathan, R. N. (2002). Characterization of chitin, chitosan and their carboxymethyl derivatives by differential scanning calorimetry. *Carbohydrate Polymers, 49*, 185–193.

Lavertu, M., Xia, Z., Serreqi, A. N., Berrada, M., Rodrigues, A., Wang, D., et al. (2003). A validated H-1 NMR method for the determination of the degree of deacetylation of chitosan. *Journal of Pharmaceutical and Biomedical Analysis, 32*, 1149–1158.

Li, W., Laurencin, C. T., Caterson, E. J., Tuan, R. S., & Ko, F. K. (2002). Electrospun nanofibrous structure: A novel scaffold for tissue engineering. *Journal of Biomedical Materials Research, 60*, 613–621.

Min, B. M., Lee, G., Kim, S. H., Nam, Y. S., Lee, T. S., & Park, W. H. (2004a). Electrospinning of silk fibroin nanofibers and its effect on the adhesion and spreading of normal human keratinocytes and fibroblasts in vitro. *Biomaterials, 25*, 1289–1297.

Min, B., Lee, S. W., Lim, J. N., You, Y., Lee, T. S., Kang, P. H., et al. (2004b). Chitin and chitosan nanofibers: Electrospinning of chitin and deacetylation of chitin nanofibers. *Polymer, 45*, 7137–7142.

Muzzarelli, R. A. A. (1993). Chitin and its derivatives: New trends of applied research. *Carbohydrate Polymers, 3*, 53–75.

Neto, C. G. T., Giacometti, J. A., Job, A. E., Ferreira, F. C., Fonseca, J. L. C., & Pereira, M. R. (2005). Thermal analysis of chitosan based networks. *Carbohydrate Polymers, 62*, 97–103.

Ohkawa, K., Cha, D., Kim, H., Nishida, A., & Yamamoto, H. (2004). Electrospinning of chitosan. *Macromolecular Rapid Communications, 25*, 1600–1605.

Percot, A., Viton, C., & Domard, A. (2003). Optimization of chitin extraction from shrimp shells. *Biomacromolecues, 4*, 12–18.

Qu, X., Wirsen, A., & Albertsson, A. C. (2000). Effect of lactic/glycolic acid side chains on the thermal degradation kinetics of chitosan derivatives. *Polymer, 41*, 4841–4847.

Rinaudo, M. (2006). Chitin and chitosan: Properties and applications. *Progress in Polymer Science, 31*, 603–632.

Tolaimate, A., Desbrieres, J., Rhazi, M., Alagui, A., Vincendon, M., & Vottero, P. (2000). On the influence of deacetylation process on the physicochemical characteristics of chitosan from squid chitin. *Polymer, 41*, 2463–2469.

Tomihata, K., & Ikada, Y. (1997). In vitro and in vivo degradation of films of chitin and its deacetylated derivatives. *Biomaterials, 18*, 567–575.

Vrieze, S. D., Westbroek, P., Camp, T. V., & Langenhove, L. V. (2007). Electrospinning of chitosan nanofibrous structures: Feasibility study. *Journal of Material Science, 42*, 8029–8034.

Wang, X., Lee, S., Drew, C., Senecal, K. J., Kumar, J., & Samuelson, L. A. (2002). Electrospun nanofibrous membranes for highly sensitive optical sensors. *Nano Letters, 2*, 1273–1275.

Wanjin, T., Cunxin, W., & Donghua, C. (2005). Kinetic studies on the pyrolysis of chitin and chitosan. *Polymer Degradation and Stability, 87*, 389–394.

Yoshimoto, H., Shin, Y. M., Terai, H., & Vacanti, J. P. (2003). A biodegradable nanofiber scaffold by elctrospinning and its potential for bone tissue engineering. *Biomaterials, 24*, 2077–2082.